Title
Longitudinal monitoring of hypertonia through a multimodal sensing glove

Authors
Liu, Jiaxi
Verrett, Mya
Wieand, Alyssa
et al.

Publication Date
2025

DOI
10.1016/j.bios.2024.116829

Peer reviewed

Biosensors and Bioelectronics 267 (2025) 116829

Contents lists available at ScienceDirect

Biosensors and Bioelectronics

journal homepage: www.elsevier.com/locate/bios

Longitudinal monitoring of hypertonia through a multimodal sensing glove

Jiaxi Liu [a], Mya Verrett [b], Alyssa Wieand [c], Anna Burch [c], Ariel Jeon [a], John Collins [c], Cagri Yalcin [e], Harinath Garudadri [f], Andrew J. Skalsky [c,d], Tse Nga Ng [a,*]

[a] Department of Electrical and Computer Engineering, University of California San Diego, La Jolla, CA, USA
[b] Shu Chien–Gene Lay Department of Bioengineering, University of California San Diego, La Jolla, CA, USA
[c] Rady Children's Hospital, San Diego, CA, USA
[d] Department of Orthopedic Surgery, University of California San Diego, La Jolla, CA, USA
[e] Electrical Engineering and Information Technology, Otto-von-Guericke University Magdeburg, Germany
[f] Qualcomm Institute, University of California San Diego, La Jolla, CA, USA

ARTICLE INFO

Keywords:
Hypertonia
Sensor glove
Neuromuscular disorders

ABSTRACT

As clinical evaluations of neuromuscular disorders such as hypertonia mostly rely on perception-based scales, the imprecise subjective ratings make it difficult to accurately monitor treatment progress. To promote objective evaluation, this work used a multi-modal sensing glove in a double-blind study to enable sensitive monitoring of medication effects across 19 participants. The biomechanical measurements from the sensing glove effectively distinguished patient cohorts receiving a baclofen treatment or a placebo with 95% confidence. Consistent monitoring over a two-month period was demonstrated, closely tracking variations in individual responses to treatment. The biomechanical changes were correlated to neural activities as recorded by electromyography, verifying the medication effects. The sensing glove is shown to be a reliable tool for point-of-care settings to facilitate precise evaluation of hypertonia, essential for tailoring individual treatment choices and timely management of chronic symptoms.

1. Introduction

Hypertonia is a chronic neuromuscular disorder manifested as an abnormal increase in muscle tone due to upper motor neuron lesions, which can arise from conditions including cerebral palsy, neurodegenerative diseases, stroke, and traumatic brain or spinal injuries. It is estimated to affect over 12 million people globally (Evans et al., 2017; Hugos and Cameron, 2019; Cherni et al., 2021). The excessive muscle tone and hyper-reflex of hypertonia impair motor control and balance, necessitating treatment to prevent exacerbation of deformities and improve the quality of life for patients. However, the monitoring of treatment progress is currently limited in precision and consistency, as most clinical evaluations are based on subjective perception ratings such as the Modified Ashworth Scale or the Tardieu Scale (Haberfehlner et al., 2020; Puzi et al., 2019; Alhusaini et al., 2010). The coarse subjective ratings hinder efforts to understand the efficacy of medication and therapies. Thus, there is a critical need to develop objective tools that can enable sensitive, consistent evaluations to facilitate evidence-based medicine and improve patient care.

To tackle the lack of objective evaluation standards, prior studies have demonstrated instrumentations that measured biomechanical properties (Wu et al., 2018; Song et al., 2018; Cherni et al., 2021; Sloot et al., 2017; Li et al., 2017; Bar-On et al., 2013) and electromyography (EMG) (Jobin and Levin, 2000; Yu et al., 2020) of muscles affected by hypertonia; but those studies were only snapshot comparisons between healthy and impaired states and did not delve into the long-term monitoring of hypertonia, which is a chronic condition. In order to show the clinical relevance of the instrumentation for consistent longitudinal assessments, this study has carried out a double-blind, randomized control trial aimed at tracking changes in 19 patients' conditions over a two-month period. This study was designed to minimize human bias, errors and placebo effect. In a double-blind study, during the treatment period neither the researcher nor the patients knew which intervention the patients were receiving. The randomized ratio was 1:1, which meant once enrolled in the study, the patient had 50% chance to be selected to receive treatment and 50% chance to be administrated the placebo. The randomized patient allocation ruled out potential bias that might affect the treatment outcome, and kept any

* Corresponding author.
E-mail address: tnn046@ucsd.edu (T.N. Ng).

https://doi.org/10.1016/j.bios.2024.116829
Received 21 May 2024; Received in revised form 12 September 2024; Accepted 30 September 2024
Available online 2 October 2024

systematic bias minimal in the study design (Sibbald and Roland, 1998). The randomization and blinding ensure that the observed change could largely be explained by the administrated treatment based on statistically significant results. This work has investigated the instrumentation capability to quantify the effect of an antispasmodic medication baclofen (Pérez-Arredondo et al., 2016; Imerci et al., 2019) and to define hypertonia severity levels, which is important for optimizing medication plans for patients.

Our instrumentation approach involves the use of a portable, multimodal sensing glove worn by the evaluator. This glove records the applied torque and motion trajectories during assessment maneuvers on patients (Amit et al., 2019, 2022; Yalcin et al., 2020; Jonnalagedda et al., 2016). In our previous demonstration, the sensing glove has been proven to effectively track muscle tone and capture the dynamic features of hypertonia, such as catch symptoms and velocity-dependent muscle resistance (Amit et al., 2022). Our design places the equipment on the evaluator instead of the patient, making it more versatile than prior biomechanical modules (Porciuncula et al., 2018; Ray et al., 2019; Haberfehlner et al., 2020) that are restricted to specific muscle types and often pose safety and clinical adoption barriers, such as poor fit to different patient sizes. The sensing glove is used to assess multiple body regions, including arms and legs. In this study, the measurements are analyzed to determine their levels of resolution and consistency in monitoring outcomes over time, enabling the differentiation of patients undergoing treatment from those receiving placebos in our double-blind study.

In addition to showing the feasibility of longitudinal monitoring, this research also seeks to further validate (Chikere et al., 2019) the sensing glove by comparing its biomechanical measurements with simultaneous EMG signals (Grippo et al., 2011). The biomechanical properties captured by the sensing glove are correlated to motor neuron activities recorded in EMG, to use two independent techniques in assessing the effects of medication. The complementary results demonstrate the potential of the sensing glove system to serve as a clinically practical standard for assessing hypertonia and enables timely interventions in managing patients' chronic symptoms and improve their quality of life.

2. Materials and methods

All measurements in this work were taken with written informed consent of the patients and their legal guardians, if applicable, and approved by UCSD Institutional Review Board #180115.

Patient Recruitment and Dosage information: The patient age ranged from 5 to 38 years old, including 9 males and 10 females. The ethnicity distribution was Hispanic 42.1%, Asian 26.3%, White 26.3%, and African American 5.3%. The patients' ages did not significantly influence the severity of hypertonia. Rather the size of the affected limbs, independent of age, had a greater influence in the force required to perform the assessment. Among the 19 patients, 16 of them were diagnosed with cerebral palsy, 1 with traumatic brain injury, 1 with Pelizaeus Mertzbacher disease, and 1 with a pineal germ cell tumor. The patient cohort covered a wide range of age, ethnicities and conditions to prevent bias. For the treatment plan, the starting dosage for all patients was 0.2 mL with 100 μg baclofen nasal solution. If the patient chose to increase their dosage on a daily basis, the baclofen dosage followed the step table in Supplemental Table S2 and the maximum dose escalation was one step every day until step 16. If they chose not to increase the dosage, they would stay at whatever dosage they deemed fit but were unable to escalate faster than one step every other day. For day 43–46, the washout period, the patient's dosage decreased to 80%, 60%,40% and 20% of the maximum dosage. Then for day 47–61, the patient stopped taking baclofen. For the placebo plan, patients took matching saline solution on the same schedule as the treatment plan.

For the pressure measurements, each limb was evaluated through at least 10 maneuvers, then the median and the standard error of the mean were computed for comparison. For the EMG signal, the baseline noise level was defined as the average of the last 1 s's recording, during which the muscles were at rest.

Clinical treatment exception: There were some data that were not collected due to missing appointments: one treatment patient's visit 1; another treatment patient's visit3; and one control patient's visit 4.

Calibration method: The glove calibration process was performed as such: we filled a 2″-diameter syringe with water to adjust the weight corresponding to multiple resistance levels, ranging from 1 to 5 lbs which were the typical for muscles with hypertonia (Lynn et al., 2014). Then, wearing the glove, the evaluator held the syringe and performed the flexion and extension maneuvers as they would on a patient's limb. The recorded pressure readings and the corresponding weights were fitted with linear regression. The calibration curve is shown in Supplemental Fig. S2 for weights 1–5 lbs. The life time of the glove is longer than ten months, proven by the sensor maps in Supplemental Fig. S2.

S.D. and S.E.M. calculation: The standard deviation S.D. was calculated with the MATLAB function 'std'. The S.E.M was calculated with the cycle numbers recorded in each set, using equation S.E.M. = S.D./$N^{0.5}$, where the sample number N was the number of maneuver cycles in the recording.

Δtorque error bar calculation: The error bars of Δtorque were determined by the standard error formula (Cote et al., 2021):

$$\mathrm{var}(\mathrm{Visit_x}, \mathrm{Visit_0}) = \sqrt{\frac{(N_x-1)^*(\mathrm{S.D._x})^2 + (N_0-1)^*(\mathrm{S.D._0})^2}{N_x+N_0-2}}^* \sqrt{\frac{1}{N_x}+\frac{1}{N_0}} \quad \text{(Eqn 1)}$$

where the subscripts denote that the data were collected at Visit(x). For example, N_x and N_0 are the number of maneuver cycles in Visit(x) and Visit(0), respectively. The variable $\mathrm{S.D._x}$ is the standard deviation of torque data in Visit(x).

T-Value calculation: The t-values in Fig. 3 were calculated with MS Excel using the built-in function found under 'Data'-'Data Analysis'-'*t*-Test: two-Sample assuming Unequal Variances'.

Test power calculation: The power in Fig. 3 was calculated post hoc based on the obtained data and sample size with software GPower version 3.1.9.7, under 'Test family-t tests. Statistical test: Difference between two independent means (two groups)'.

Surface EMG: The surface EMG signals were collected using the Delsys Trigno System with Avanti Sensors shown in Supplemental Fig. S2. The sensors were adhered to participants with double-sided tape. The EMG signal was sampled at 2000Hz and no filter was applied during the recording process.

EMG coactivation time calculation: The EMG signals were filtered by a 5th order high-pass Butterworth filter at a cutoff frequency of 10 Hz. Then the signals were normalized with the 'normalize' function in MATLAB. To determine the muscle activation state from the EMG signal, the signal's envelope was compared to the baseline noise level. The baseline noise level was defined as the average of the last 1 s's recording, during which the muscles were at rest. For the signal envelope, a sliding window of 50 datapoints was used to calculate the root-mean-square envelopes. When the signal envelope was higher than the defined noise level continuously for 30 data points (equivalent to 0.015 s), the period was considered 'on', in which the muscle was activated. Otherwise, the period was considered as 'off' with no significant muscle activation. The CoD was computed by determining the overlapping duration during which a pair of muscles were both in the 'on' activated state, divided by the entire flexion/extension phase duration.

3. Results and discussion

3.1. Study design

The abnormal muscle tone of hypertonia, as illustrated in Fig. 1A, is evaluated by using the sensing glove to measure the torque exerted to

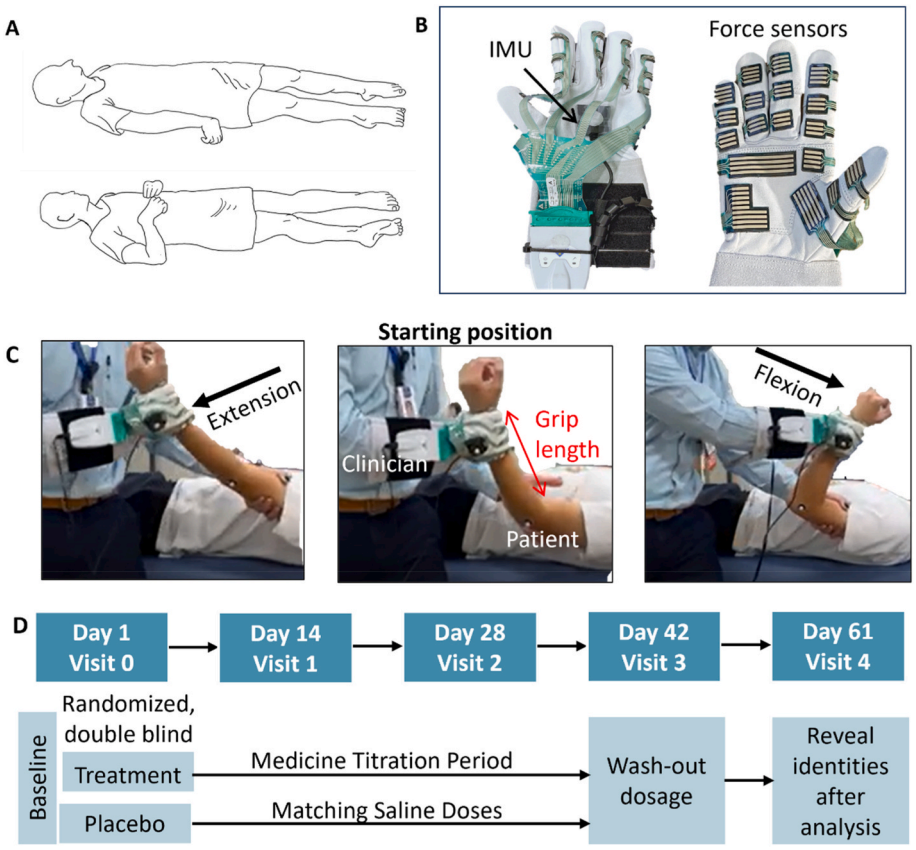

Fig. 1. Measurement protocols. (A) Illustrations of abnormal muscle tone in hypertonia. (B) The multimodal sensing glove with an inertial measurement unit and force sensors. (C) To assess hypertonia, the clinician wore the sensing glove to record the patient's muscle tone while performing extension and flexion maneuvers on the patient's limbs. (D) Schedule and design of this double-blind study to objectively monitor patient condition using the sensing glove.

move the patient's affected muscles. A higher torque indicates increased muscle tone (namely, resistance to movement) and more severe hypertonia. The multi-modal sensing glove (Amit et al., 2022) in Fig. 1B has 349 force-sensitive resistors (Tekscan Inc.) on the palm side and an inertial measurement unit (IMU from MotionNode Inc.) on the back side. The synchronized sensors would simultaneously acquire the muscle tone and the maneuver trajectories, capturing the dynamic characteristics of hypertonic muscles, i.e., velocity-dependent muscle resistance.

In the evaluation procedure as shown in Fig. 1C, the clinician wore the sensor glove to perform standardized flexion and extension maneuvers on patients, as normally done in perception-based clinical evaluations. The patient remained passive in a supine position and voluntary motion was not required from the patient, because the patient might be physically and/or cognitively unable to follow instructions. Throughout the maneuvers, the clinician would stabilize the patient's joint with one hand, and then the gloved hand would move the patient's limb through eight to ten cycles, striving to reach a steady level in the cycling measurements. In this study, each patient was evaluated on all four limbs, including the elbows and knees on the left and right sides.

Through the double-blind experiment, we ensured that the observed changes in patients' muscle tone were determined without influence from perception biases. The results would establish whether the glove measurements can function as objective, sensitive metrics for assessing treatment effects. This study monitored 19 patients, who were randomly assigned to two groups. One group received the antispasmodic baclofen medication, while the other received a saline placebo delivered in the same manner as the baclofen. The patients were measured five times following the schedule in Fig. 1D. At the initial Visit 0, the clinician recorded each patient's baseline condition and provided them with doses of either baclofen or placebo for daily consumption over a two-week period. Then, the patients returned biweekly for evaluation and to receive continual dosages. To mitigate the potential for baclofen to induce sudden withdrawal symptoms (Pérez-Arredondo et al., 2016; Imerci et al., 2019; Boster et al., 2016; Skalsky and Fournier, 2015), the dosage dispensed at Visit 3 was designed to gradually reduce the medication to zero in a washout period. By Visit 4, all the patients were no longer taking any dosage and underwent a final evaluation. It was only after the completion of data analysis that the group assignments were revealed.

3.2. Maneuver analysis

Fig. 2A displays a representative recording of the evaluation maneuvers performed on a patient's limb. The processing of sensor signals to obtain the angular velocity and torque data are discussed in our previous publication (Amit et al., 2022) and in the Experimental Methods section. In brief, the angular velocity along the axis of maximum motion was determined through applying principal component analysis on the data taken from the 3-axis gyroscope in the IMU. For the torque measurement, signals from all the force sensor pixels (shown in the inset of Fig. 2A) were summed together at each sampling time point. The relation $\tau = \ell \times F = \ell F \sin\theta$ was used to calculate the torque τ from the summed force F. The grip length ℓ was measured between the patient's joint and the location where the clinician gripped the patient's limb, as denoted by the red line in Fig. 1C. The angle θ was presumed to be 90° [$\sin(90°) = 1$], since the clinician applied force in the direction perpendicular to the grip length.

The 10-s recording of angular velocity and torque in Fig. 2A shows 8 maneuver cycles. For these synchronized signals, each cycle can be further segmented to uncover the variations in muscle resistance under

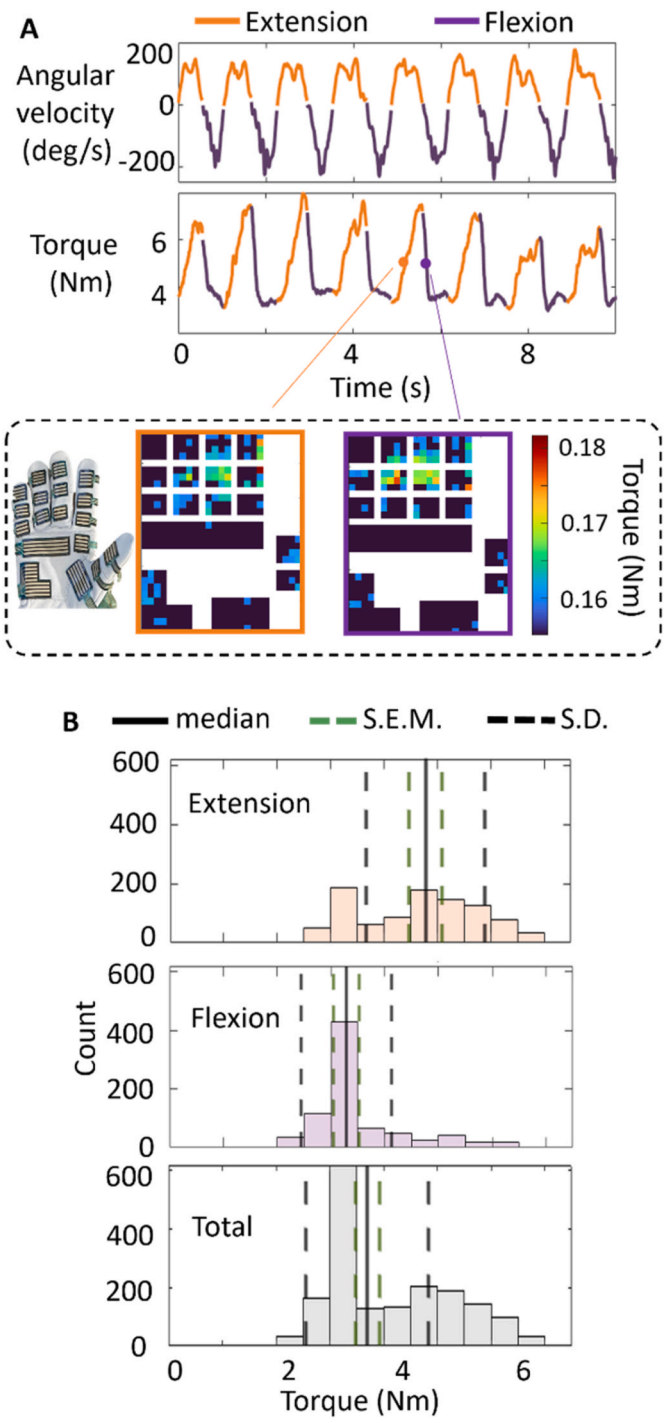

Fig. 2. An exemplar measurement taken on a patient's right elbow. (A) Angular velocity and torque versus time. The torque was calculated from summing all the activated sensor pixels at each sampling time point. Inside the dashed box: spatial maps of activated sensors under extension (orange) and flexion (purple) at the marked time points. (B) Histograms of the torque measurements from part A, corresponding to extension or flexion segments, and the total sum.

flexion and extension. Because the maneuver velocity must drop to zero in order to switch movement directions between flexion and extension, the zero-crossing points within the angular velocity data indicated the endpoints of each flexion/extension segment. Using the corresponding time points where v = 0°/s, the torque measurements were demarcated into flexion (purple) and extension (orange) segments. This segmented torque data highlighted the asymmetric tone between the extensor and flexor muscles, as clearly evident in the corresponding histograms in Fig. 2B. The torque histogram for extension segments presented a higher median value compared to that under flexion. When there was more stiffness in a patient's muscle, the evaluator had to apply an increased torque to overcome the patient's muscle resistance. The higher torque median signified worse hypertonia in the muscles engaged in extension. The unequal muscle tone suggests different degrees of damage to the two brain hemispheres (Chen et al., 2020; Straathof et al., 2022) and is quite common; specifically among our evaluation trials, with over 10% of the results exhibiting asymmetric muscle tone (Supplemental Table S1). However, considering that our study used systemic baclofen, rather than a localized treatment such as botox injections (Esquenazi et al., 2013; Deltombe et al., 2019), our next analysis would focus on the total torque datasets without segmentation. Afterwards, we will return to use the segmentation process for comparison with EMG in the final section of this study.

3.3. Comparison of patient cohorts under baclofen treatment and placebo

As described earlier, the patients were evaluated five times over a two month period. After each visit, the torque histograms were extracted from the recordings, typically encompassing eight to ten maneuver cycles. For the histograms, various statistical measures were determined, such as the median, standard deviation (S.D.), and standard error of the mean (S.E.M.). The dashed black lines in the histograms denote ±1 S.D. of the dataset. The dashed green lines mark the S.E.M (Wan et al., 2014). To quantify the changes in muscle tone between visits, the median values in the histograms were used to calculate a metric defined as Δtorque:

Δtorque of Visit(x) = torque median at Visit(x) – torque median at Visit (0) (Eqn 2)

The Δtorque represents the change in muscle tone with respect to the initial baseline condition and accounts for cumulative effects from the medication, if any, over the duration of the study. A negative Δtorque means a decreased resistance to movement, namely the patient's muscle tone has reduced to a lower severity compared to their baseline, and conversely for a positive value of Δtorque.

Fig. 3A and B displays opposite shifts in the torque histograms from Visit 0 to Visit 4 for two different patients. Upon revealing the group assignments, it was confirmed that the data of Fig. 3A were taken on a patient in the treatment group receiving baclofen medication, whereas those of Fig. 3B were from a patient in the placebo group. These results aligned with the notion that baclofen would have treatment effects of reducing muscle tone, leading to a negative Δtorque for the patient receiving the medication. Whereas for the patient on the placebo, the muscle tone did not improve and even slightly worsened over time, as evidenced by the positive Δtorque indicating the lack of treatment effect. Meanwhile, the clinical Modified Ashworth Scale (MAS) scores were rated to be the same, at 1.5 out of the scale of 4, for all the visits and showed no clear trend to distinguish the medication effect. The insensitive MAS scores underscored the difficulty in using a perception-based scale to monitor treatment outcomes.

For our double-blind study which included 11 patients in the treatment group and 8 patients in the placebo group, the Δtorque metrics for every patient are summarized in Fig. 3C, where each bar in the same row represents the same patient (Esquenazi et al., 2013). While the variance values ranged from 1 to 5 Nm, on average ± 1 Nm was the typical torque resolution of the sensing glove for detecting changes in muscle tone.

Fig. 3C is very rich in information, revealing key insights when comparing the outcomes between cohorts and within individuals. Regarding the difference between the treatment and placebo cohorts, the patients under treatment (blue bars) all showed Δtorque progressing towards negative values by Visit 3. Subsequently following the washout period, the treatment group still retained some improvement in muscle

tone at the final Visit 4. In contrast, the Δtorque of patients receiving placebos (white bars) fluctuated around zero, with some displayed a tendency towards positive values that indicated worsening muscle tone over time, while others bounced between small ± values with no clear pattern.

To evaluate the difference between the Δtorque distributions of the treatment and placebo groups, unpaired t-tests were performed and established that the difference was statistically significant at the confidence level of 95%. In this work the critical t-value was 1.9 as determined from the sample degrees of freedom of 17. Since all the calculated t-values, as shown in Fig. 3C, exceeded this critical threshold of 1.9, the *t*-test results demonstrated that the Δtorque distribution between the treatment and placebo groups were statistically different across all visits. In addition to t-values, another important statistical parameter was the test power, denoted as (1-β), which was calculated post-hoc with the tool G*Power version 3.1.9.7 (Faul et al., 2007; Sakpal, 2010). The (1-β) value represented the probability of "true positive", and a power value higher than 0.8 is conventionally considered to be adequate. For the data in Fig. 3C, all the power values exceeded 0.92, providing reassurance that the study sample size was sufficient in our analyses.

Thus, two important findings were drawn from Fig. 3C. First, between the treatment and placebo cohorts, the glove data distinguished the medication efficacy within the studied populations. Second, on an individual level, the glove provided consistent monitoring over time with a resolution down to ±1 Nm, facilitating the sensitive detection of variations in individual responses to treatment. Hence, the measurement results can be used to tailor and optimize personalized medication plans for each patient, beneficial for mitigating side effects and promoting timely interventions, which would be especially valuable for pediatric patients experiencing rapid growth and development.

3.4. Comparison of measurements from electromyography and sensing glove

While the above measurements focused on assessing the biomechanical changes in muscle tone, the abnormality of hypertonic muscles is also correlated with hyperactivities of motor neurons (Van Der Krogt et al., 2015), in which the imbalance between excitatory and inhibitory control hindered the muscle from executing fluid coordinated movement and resulting in exaggerated resistance. The electrical signals from motor neurons have been captured by surface EMG for evaluation of motor disorders based on the muscle co-activation characteristics (Xie

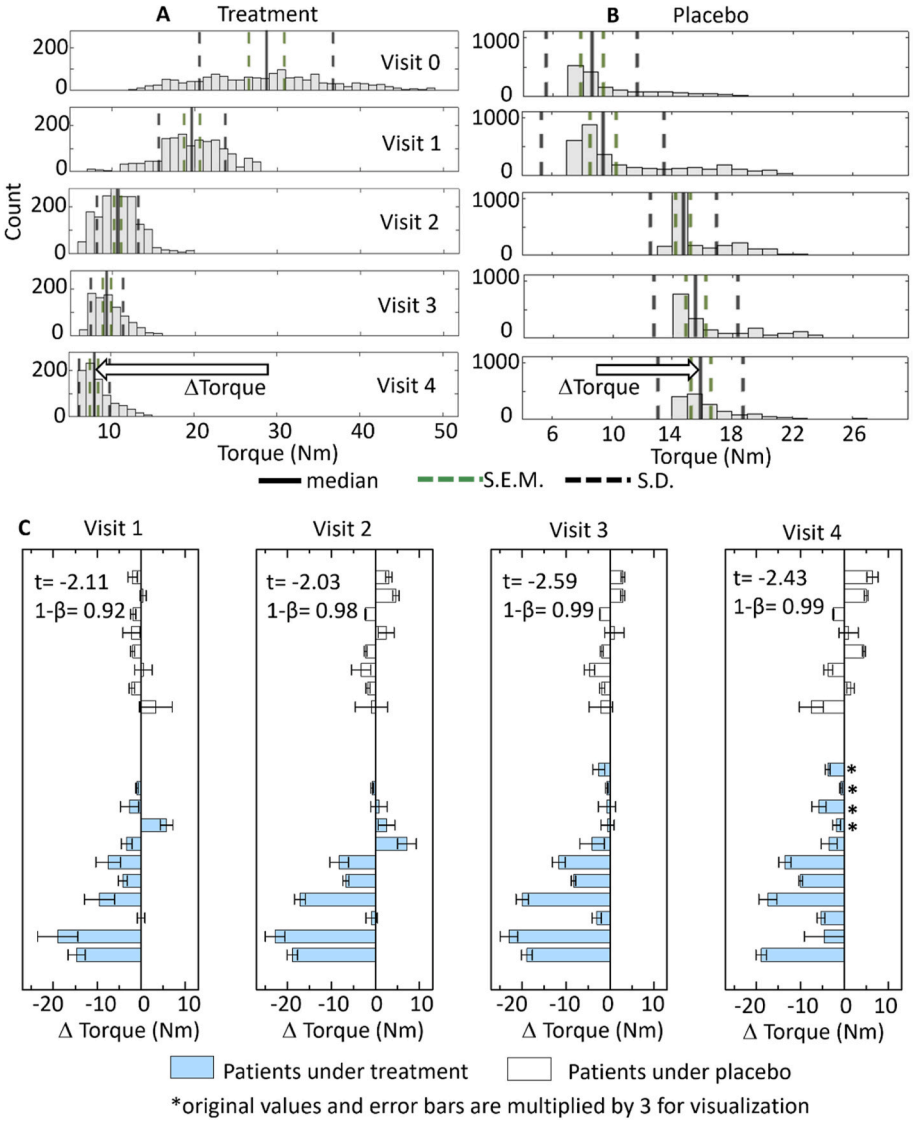

Fig. 3. Comparison of torque histograms over multiple visits. ΔTorque denotes the change of the median torque between the initial visit 0 and later visits. Example data of (A) a patient receiving medication and (B) a patient taking the placebo. (C) Summary of Δtorque across all visits. Each bar in the same row represents the same patient.

et al., 2020; Hu et al., 2018; Ricciardi et al., 2020; Chow and Stokic, 2020). Therefore, we carried out a double-blind test that incorporated surface EMG as a complementary technique to validate the biomechanical readings of the sensing glove. This test was conducted on two patients to compare treatment and placebo outcomes, following the biweekly evaluation and dosage schedule up to Visit 3, as depicted in Fig. 1D, and with simultaneous EMG and sensing glove recordings. The experimental setup is shown in Fig. 4A, where EMG sensors were placed on a pair of agonist and antagonist muscles, specifically the biceps and triceps of the patient's arm. The EMG and sensing glove systems were synchronized to simultaneously capture data as the patient's arm was moved to flexion and extension positions.

To interpret the EMG data, prior studies have introduced a metric of co-activation duration (CoD) (Chow and Stokic, 2020), where CoD was computed by determining the overlapping duration during which a pair of muscles were both active, divided by the entire flexion/extension phase duration. The muscles being examined should be an agonist-antagonist pair, such as biceps-triceps on the upper arm or quadriceps-hamstring on the upper leg. In a healthy person, the EMG of an agonist-antagonist muscle pair showed alternating activation of each muscle (Ueyama, 2021). In contrast, the EMG of a patient with hypertonia displayed frequent co-activation as illustrated in Fig. 4B, such that the bursts of neuron firings were concurrent in both muscles and would interfere with each other.

The muscles were considered active when the EMG amplitude exceeded the noise level of the baseline for at least 15 ms. The EMG magnitudes were not correlated to the applied torque and were notoriously prone to issues with environmental noises and reproducibility due to variations in electrode locations and skin conductivity. However, the EMG CoD showed better repeatability than magnitudes and therefore were selected for comparison with the torque measurements from the sensing glove. At times, the phase duration was not clear-cut based solely on EMG data; but the simultaneous velocity measurements from the glove could be used to better define segmentation of flexion and extension phases as done in Fig. 2A. Since the EMG and the glove data were collected simultaneously, the agonist and antagonist muscles should activate alternatively corresponding to the extension and flexion direction maneuver. The angle of the glove and the time at which the direction switched were recorded by the IMU. The phase durations obtained from the IMU data were then employed to reduce the uncertainties in the denominators when calculating the CoD.

Fig. 4C and D compares the data collected on each patient's right elbow, with one patient under treatment and the other under placebo, respectively. During the initial Visit 0, both patients showed a CoD >50%, manifesting abnormal co-activation. For the patient under baclofen treatment in Fig. 4C, both the EMG and glove measurements showed the same trend, with the CoD and median torque dropped as treatment progressed. By Visit 3, the CoD was only 10%, and the median

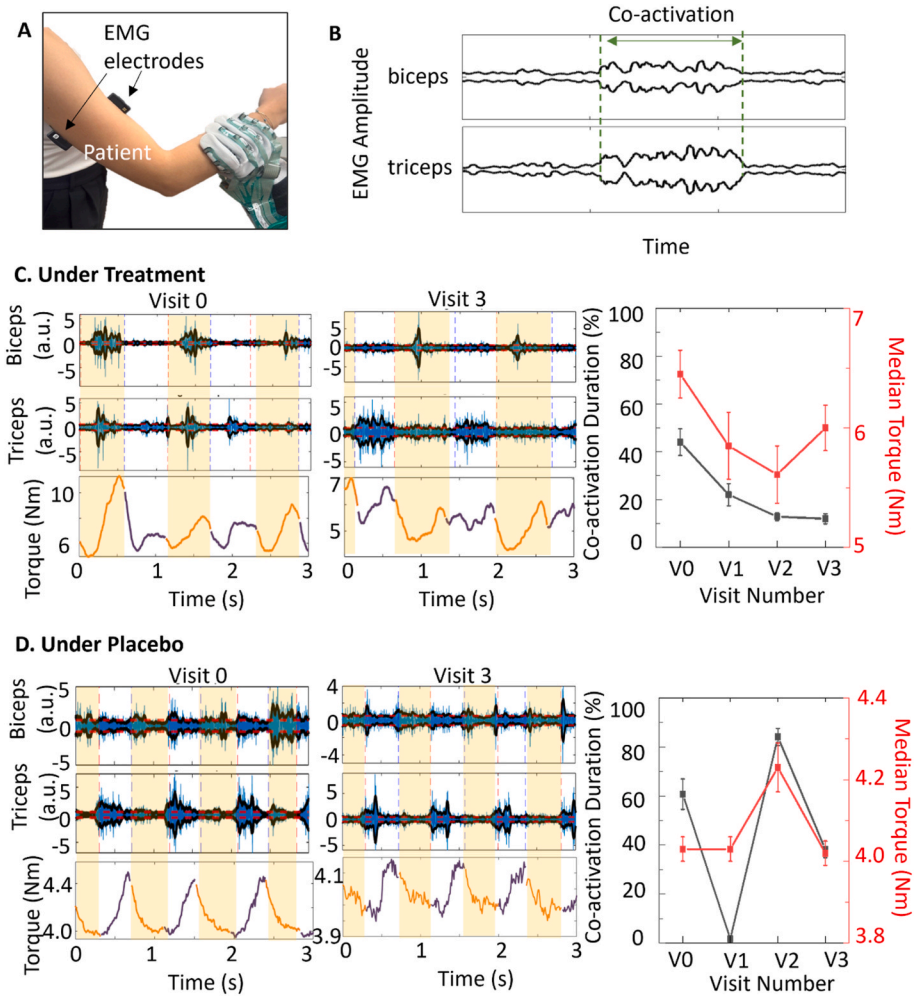

Fig. 4. Simultaneous EMG and sensing glove measurements. (A) Photograph of the EMG sensor locations on a patient's arm. (B) Illustration of the muscle coactivation period. (C) Simultaneous measurements of EMG on biceps and triceps muscles and the torque required to move the patient's arm. The exemplar data were taken at Visit 0 and Visit 3. The shaded and unshaded areas indicate the muscle under extension and flexion, respectively. The graph on the right presents the EMG coactivation duration and the median torque at each visit. The error bars correspond to the S.E.M. calculated from all the maneuver cycles.

torque was also lower than the initial resistance in Visit 0. These measurements were in agreement and indicated improvement of hypertonia symptoms under treatment. Whereas for the patient under placebo, both the CoD and median torque fluctuated but did not show improvement between Visits 0 and 3. Overall, the trends in the EMG and biomechanical measurements were generally consistent and mutually validated the medication effects.

The EMG and the sensing glove provided complementary views of mechanical and neural aspects in hypertonia. Nonetheless, we note that the torque data offered a more direct mechanical characterization of muscle resistance. On its own, the easy-to-use sensing glove can serve a stand-alone standard for point-of-care settings to facilitate precise evaluation of treatment outcomes.

3.5. Limitations of the study

The study has two limitations to be addressed in future research. The first is that the evaluation maneuvers engaged only gross-motor movements for the arms and legs, and it would be desirable to extend the evaluation to muscles involved in fine-motor movements, such as wrist and ankle protonation and supination. In these fine-motor maneuvers, the torque generated would be lower than that of larger limbs and might require an enhancement of the force sensors' detection limit in in order to accurately measure these movements. The second limitation is that the system needed individual calibration for each rater, done by the maneuvering dumbbells from 1 to 5 lb to correlate sensor outputs with known weights. The measurements here were done by the same clinician (Dr. Skalsky), and we did not examine the consistency in measurements across different raters. The inter-rater reproducibility should be evaluated in the future, and any potential discrepancies can likely be mitigated through calibration and signal processing techniques such as neural-network supervised learning (Yalcin et al., 2020) to standardize the results across different raters. The standardization will help to increase the number of people able to measure patients suffering from hypertonia, for example to enable at-home assessments by caregivers to facilitate telemedicine and extend care to patients with limited access to rehabilitation specialists.

4. Conclusion

This report demonstrates precise longitudinal monitoring of baclofen medication efficacy in treating hypertonia through a portable multimodal sensing glove. In our double-blind study, the biomechanical measurements yielded results that effectively distinguished between patient cohorts and closely tracked changes within individual patients. Moreover, this study validated the biomechanical glove system with neural EMG, establishing the glove metrics as a reliable standard for hypertonia evaluations even in noisy point-of-care settings.

The highly sensitive measurements readily showed treatment outcomes during biweekly evaluations, eliminating the need for long waiting periods. This capability would be critical for identifying potential problems during treatment; for instance, a study of intrathecal baclofen treatment determined that 19.7% of the cases encountered medication delivery problems to the target sites (Imerci et al., 2019). Objective assessments through the sensing glove can indicate when the efficacy of a treatment was low and promote timely intervention. In turn, this added measure can lead to savings on medication costs, minimize delays in managing chronic symptoms, and ultimately enhance the quality of life for patients.

CRediT authorship contribution statement

Jiaxi Liu: Writing – original draft, Visualization, Methodology, Formal analysis, Data curation. **Mya Verrett:** Software, Data curation. **Alyssa Wieand:** Methodology, Investigation. **Anna Burch:** Writing – review & editing, Investigation. **Ariel Jeon:** Software, Data curation. **John Collins:** Methodology. **Cagri Yalcin:** Software. **Harinath Garudadri:** Software. **Andrew J. Skalsky:** Supervision, Methodology, Conceptualization. **Tse Nga Ng:** Writing – review & editing, Supervision, Funding acquisition, Formal analysis, Conceptualization.

Declaration of competing interest

The authors declare the following financial interests/personal relationships which may be considered as potential competing interests: Tse Nga Ng, Andrew Skalsky, Harinath Garudadri have patent #US-11123013-B2 issued to Nadi. If there are other authors, they declare that they have no known competing financial interests or personal relationships that could have appeared to influence the work reported in this paper.

Data availability

Data will be made available on request.

Acknowledgments

J.L., M.V., A.J., A.J.S., and T.N.N. are grateful for the support from the National Science Foundation CBET#2054517.

Appendix A. Supplementary data

Supplementary data to this article can be found online at https://doi.org/10.1016/j.bios.2024.116829.

References

Alhusaini, A.A., Dean, C.M., Crosbie, J., Shepherd, R.B., Lewis, J., 2010. Evaluation of spasticity in children with cerebral palsy using Ashworth and Tardieu Scales compared with laboratory measures. J. Child Neurol. 25, 1242–1247.

Amit, M., Chukoskie, L., Skalsky, A.J., Garudadri, H., Ng, T.N., 2019. Flexible pressure sensors for objective assessment of motor disorders. Adv. Funct. Mater., 1905241

Amit, M., Yalcin, C., Liu, J., Skalsky, A.J., Garudadri, H., Ng, T.N., 2022. Multimodal assessment of spasticity using a point-of-care instrumented glove to separate neural and biomechanical contributions. iScience 25, 105286.

Bar-On, L., Aertbeliën, E., Wambacq, H., Severijns, D., Lambrecht, K., Dan, B., Huenaerts, C., Bruyninckx, H., Janssens, L., Van Gestel, L., Jaspers, E., Molenaers, G., Desloovere, K., 2013. A clinical measurement to quantify spasticity in children with cerebral palsy by integration of multidimensional signals. Gait Posture 38, 141–147.

Boster, A.L., Adair, R.L., Gooch, J.L., Nelson, M.E.S., Toomer, A., Urquidez, J., Saulino, M., 2016. Best practices for intrathecal baclofen therapy: dosing and long-term management. Neuromodulation 19, 623–631.

Chen, B., Sangari, S., Jakob Lorentzen, X., Nielsen, J.B., Perez, M.A., Bilat, P.M., 2020. Bilateral and asymmetrical contributions of passive and active ankle plantar flexors stiffness to spasticity in humans with spinal cord injury. J. Neurophysiol. 124, 973–984.

Cherni, Y., Ballaz, L., Girardin-Vignola, G., Begon, M., 2021. Intra- and inter-tester reliability of spasticity assessment in standing position in children and adolescents with cerebral palsy using a paediatric exoskeleton. Disabil. Rehabil. 43, 1001–1007.

Chikere, C.M.U., Wilson, K., Graziadio, S., Vale, L., Allen, A.J., 2019. Diagnostic test evaluation methodology: a systematic review of methods employed to evaluate diagnostic tests in the absence of gold standard - an update. PLoS One 14, e0223832.

Chow, J.W., Stokic, D.S., 2020. Relations between knee and ankle muscle coactivation and temporospatial gait measures in patients without hypertonia early after stroke. Exp. Brain Res. 238, 2909–2919.

Cote, L.R., Gordon, R., Randell, C.E., Schmitt, J., Marvin, H., 2021. Introduction to statistics in the psychological sciences. Open Educational Resources Collection. https://irl.umsl.edu/oer/25-Version08/01/2023.

Deltombe, T., Lejeune, T., Gustin, T., 2019. Botulinum toxin type A or selective neurotomy for treating focal spastic muscle overactivity? Ann Phys Rehabil Med 62, 220–224.

Esquenazi, A., Albanese, A., Chancellor, M.B., Elovic, E., Segal, K.R., Simpson, D.M., Smith, C.P., Ward, A.B., 2013. Evidence-based review and assessment of botulinum neurotoxin for the treatment of adult spasticity in the upper motor neuron syndrome. Toxicon 67, 115–128.

Evans, S.H., Cameron, M.W., Michael Burton, J., 2017. Hypertonia. Curr. Probl. Pediatr. Adolesc. Health Care 47, 161–166.

Faul, F., Erdfelder, E., Lang, A.-G., Buchner, A., 2007. G*Power 3: a flexible statistical power analysis program for the social, behavioral, and biomedical sciences. Behav. Res. Methods 39, 175–191.

Grippo, A., Carrai, R., Hawamdeh, Z., Falsini, C., Aito, S., Pinto, F., De Scisciolo, G., Pizzi, A., 2011. Biomechanical and electromyographic assessment of spastic

hypertonus in motor complete traumatic spinal cord-injured individuals. Spinal Cord 49, 142–148.
Haberfehlner, H., Goudriaan, M., Bonouvrié, L.A., Jansma, E.P., Harlaar, J., Vermeulen, R.J., Van Der Krogt, M.M., Buizer, A.I., 2020. Instrumented assessment of motor function in dyskinetic cerebral palsy: a systematic review. BioMed Central Ltd. [Preprint]. https://doi.org/10.1186/s12984-020-00658-6.
Hu, B., Zhang, X., Mu, J., Wu, M., Zhu, Z., Liu, Z., Wang, Y., 2018. Spasticity measurement based on the hht marginal spectrum entropy of sEMG using a portable system: a preliminary study. IEEE Trans. Neural Syst. Rehabil. Eng. 26, 1424–1434.
Hugos, C.L., Cameron, M.H., 2019. Assessment and measurement of spasticity in MS: state of the evidence. Curr. Neurol. Neurosci. Rep. 19, 79.
Imerci, A., Rogers, K.J., Pargas, C., Sees, J.P., Miller, F., 2019. Identification of complications in paediatric cerebral palsy treated with intrathecal baclofen pump: a descriptive analysis of 15 years at one institution. J Child Orthop 13, 529–535.
Jobin, A., Levin, M.F., 2000. Regulation of stretch reflex threshold in elbow flexors in children with cerebral palsy: a new measure of spasticity. Dev. Med. Child Neurol. 42, 531–540.
Jonnalagedda, P., Deng, F., Douglas, K., Chukoskie, L., Yip, M., Ng, T.N., Nguyen, T., Skalsky, A., Garudadri, H., 2016. An instrumented glove for improving spasticity assessment. IEEE Healthcare Innovation Point-of-Care Technologies Conference, pp. 167–170.
Li, X., Shin, H., Li, S., Zhou, P., 2017. Assessing muscle spasticity with Myotonometric and passive stretch measurements: validity of the Myotonometer. Sci. Rep. 7, 44022.
Lynn, B.O., Van Campenhout, A., Kaat, D., Erwin, A., Huenaerts, C., Vandendoorent, B., Nieuwenhuys, A., Molenaers, G., Bar-On, L., Van Campenhout, A., Desloovere, K., Aertbeliën, E., Huenaerts, C., Vandendoorent, B., Nieuwenhuys, A., Molenaers, G., 2014. Is an instrumented spasticity assessment an improvement over clinical spasticity scales in assessing and predicting the response to integrated botulinum toxin type A treatment in children with cerebral palsy? Arch. Phys. Med. Rehabil. 95, 515.
Pérez-Arredondo, A., Cázares-Ramírez, E., Carrillo-Mora, P., Martínez-Vargas, M., Cárdenas-Rodríguez, N., Coballase-Urrutia, E., Alemón-Medina, R., Sampieri, A., Navarro, L., Carmona-Aparicio, L., 2016. Baclofen in the therapeutic of sequele of traumatic brain injury: spasticity. Clin. Neuropharmacol. 39, 311–319.
Porciuncula, F., Roto, A.V., Kumar, D., Davis, I., Roy, S., Walsh, C.J., Awad, L.N., 2018. Wearable movement sensors for rehabilitation: a focused review of technological and clinical advances. Pharm. Manag. PM R 10, S220–S232.
Puzi, A.A., Sidek, S.N., Khairuddin, I.M., Md Yusof, H., Mat Rosly, H., 2019. Inter-rater and intra-rater reliability of quantitative upper limb spasticity evaluation based on modified ashworth scale tool. In: 2018 IEEE EMBS Conference on Biomedical Engineering and Sciences, IECBES 2018 - Proceedings, pp. 126–130.
Ray, T.R., Choi, J., Bandodkar, A.J., Krishnan, S., Gutruf, P., Tian, L., Ghaffari, R., Rogers, J.A., 2019. Bio-integrated wearable systems: a comprehensive review. Chem Rev 119, 5461–5533.
Ricciardi, C., Iuppariello, L., Ricciardelli, G., Amboni, M., Cesarelli, G., Improta, G., D'Addio, G., Cannaviello, G., 2020. A quantitative analysis of muscular co-activation on EMG signals in spastic patients treated with Botulinum toxin. In: IEEE International Symposium on Medical Measurements and Applications. IEEE, p. 978.
Sakpal, T.V., 2010. Sample size estimation in clinical trial. PICR 1, 67–69.
Sibbald, B., Roland, M., 1998. Understanding controlled trials: why are randomised controlled trials important? BMJ 316, 201, 201.
Skalsky, A.J., Fournier, C.M., 2015. Intrathecal baclofen bolus dosing and catheter tip placement in pediatric tone management. Phys Med Rehabil Clin N Am 26, 89–93.
Sloot, L.H., Bar-On, L., van der Krogt, M.M., Aertbeliën, E., Buizer, A.I., Desloovere, K., Harlaar, J., 2017. Motorized versus manual instrumented spasticity assessment in children with cerebral palsy. Dev. Med. Child Neurol. 59, 145–151.
Song, S.Y., Pei, Y., Tippett, S.R., Lamichhane, D., Zallek, C.M., Hsiao-Wecksler, E.T., 2018. Validation of a wearable position, velocity, and resistance meter for assessing spasticity and rigidity. Frontiers in Biomedical Devices - 2018 Design of Medical Devices Conference, pp. 6–9.
Straathof, E.J.M., Hamer, E.G., Hensens, K.J., La Bastide – van Gemert, S., Heineman, K. R., Hadders-Algra, M., 2022. Development of muscle tone impairments in high-risk infants: associations with cerebral palsy and cystic periventricular leukomalacia. Eur. J. Paediatr. Neurol. 37, 12–18.
Ueyama, Y., 2021. Costs of position, velocity, and force requirements in optimal control induce triphasic muscle activation during reaching movement. Sci. Rep. 11, 16815.
Van Der Krogt, H., Klomp, A., De Groot, J.H., De Vlugt, E., Van Der Helm, F.C.T., Meskers, C.G.M., Arendzen, J.H., 2015. Comprehensive neuromechanical assessment in stroke patients: reliability and responsiveness of a protocol to measure neural and non-neural wrist properties. J. NeuroEng. Rehabil. 12, 1–10.
Wan, X., Wang, W., Liu, J., Tong, T., 2014. Estimating the sample mean and standard deviation from the sample size, median, range and/or interquartile range. BMC Med. Res. Methodol. 14, 135.
Wu, Y.N., Park, H.S., Chen, J.J., Ren, Y., Roth, E.J., Zhang, L.Q., 2018. Position as well as velocity dependence of spasticity- four-dimensional characterizations of catch angle. Front. Neurol. 9, 863.
Xie, T., Leng, Y., Zhi, Y., Jiang, C., Tian, N., Luo, Z., Yu, H., Song, R., 2020. Increased muscle activity accompanying with decreased complexity as spasticity appears: high-density EMG-based case studies on stroke patients. Front. Bioeng. Biotechnol. 8, 589321.
Yalcin, C., Sam, M., Bu, Y., Amit, M., Skalsky, A., Yip, M., Ng, T.N., Garudadri, H., 2020. Artifacts mitigation in sensors for spasticity assessment. Advanced Intelligent Systems, 2000106.
Yu, S., Chen, Y., Cai, Q., Ma, K., Zheng, H., Xie, L., 2020. A novel quantitative spasticity evaluation method based on surface electromyogram signals and adaptive neuro fuzzy inference system. Front. Neurosci. 14, 462.